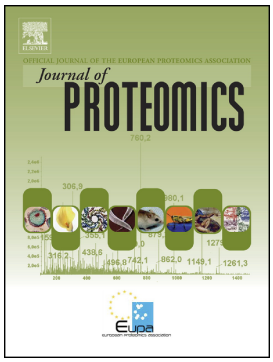

Proteome profile of neutrophils from a transgenic diabetic pig model shows distinct changes

Maria Weigand, Roxane L. Degroote, Barbara Amann, Simone Renner, Eckhard Wolf, Stefanie M. Hauck, Cornelia A. Deeg

PII: S1874-3919(20)30211-6

DOI: https://doi.org/10.1016/j.jprot.2020.103843

Reference: JPROT 103843

To appear in: *Journal of Proteomics*

Received date: 26 February 2020

Revised date: 13 May 2020

Accepted date: 23 May 2020

Please cite this article as: M. Weigand, R.L. Degroote, B. Amann, et al., Proteome profile of neutrophils from a transgenic diabetic pig model shows distinct changes, *Journal of Proteomics* (2019), https://doi.org/10.1016/j.jprot.2020.103843

Proteome profile of neutrophils from a transgenic diabetic pig model shows distinct changes

Maria Weigand[1], Roxane L. Degroote[1], Barbara Amann[1], Simone Renner[2,3,4], Eckhard Wolf[2,3,4,5], Stefanie M. Hauck[6], Cornelia A. Deeg[1,*] Cornelia.Deeg@lmu.de

[1]Chair of Pshysiology, Department of Veterinary Sciences, LMU Munich, Germany

[2]Chair for Molecular Animal Breeding and Biotechnology, Gene Center and Department of Veterinary Sciences, LMU Munich, Germany

[3]Center for Innovative Medical Models (CiMM), Department of Veterinary Sciences, LMU Munich, Germany

[4]German Center for Diabetes Research (DZD), Neuherberg, Germany

[5]Laboratory for Functional Genome Analysis (LAFUGA), Gene Center, LMU Munich, Germany

[6]Research Unit Protein Science, Helmholtz Center Munich, German Research Center for Environmental Health GmbH, Germany

*Corresponding author.

This work was supported by grants from the Deutsche Forschungsgemeinschaft SPP project 2127 DFG DE 719/7-1 (to C.D.) and HA 6014/5-1 (to S.M.H.).

ABSTRACT

INS^{C94Y} transgenic pigs develop a stable diabetic phenotype early after birth and therefore allow studying the influence of hyperglycemia on primary immune cells in an early stage of diabetes mellitus *in vivo*. Since immune response is altered in diabetes mellitus, with deviant neutrophil function discussed as one of the possible causes in humans and mouse models, we investigated these immune cells in *INS*^{C94Y} transgenic pigs and wild type controls at protein level. A total of 2371 proteins were quantified by label-free LC-MS/MS. Subsequent differential proteome analysis of transgenic animals and controls revealed clear differences in protein abundances, indicating a deviant behavior of

granulocytes in the diabetic state. Interestingly, abundance of myosin regulatory light chain 9 (MLC-2C) was increased 5-fold in cells of diabetic pigs. MLC-2C directly affects cell contractility by regulating myosin ATPase activity, can act as transcription factor and was also associated with inflammation. It might contribute to impaired neutrophil cell adhesion, migration and phagocytosis.

Our study provides novel insights into proteome changes in neutrophils from a large animal model for permanent neonatal diabetes mellitus and points to dysregulation of neutrophil function even in an early stage of this disease.

Data are available via ProteomeXchange with identifier PXD017274.

SIGNIFICANCE

Our studies provide novel basic information about the neutrophil proteome of pigs and contribute to a better understanding of molecular mechanisms involved in altered immune cell function in an early stage diabetes. We demonstrate proteins that are dysregulated in neutrophils from a transgenic diabetic pig and have not been described in this context so far. The data presented here are highly relevant for veterinary medicine and have translational quality for diabetes in humans.

KEYWORDS

Quantitative label-free LC-MS/MS; diabetes mellitus; neutrophil; granulocyte; transgenic pig; myosin regulatory light chain 9 (MLC-2C)

INTRODUCTION

With increasing prevalence in both developed and developing countries, diabetes mellitus has become the most important metabolic disease in humans today [1, 2]. A link between diabetes and increased susceptibility for infections was proven by numerous studies [3]. In addition to this, severe courses of disease like bacteremia are seen more often in diabetic patients than in people with no disease history [4]. While clinical importance of these findings is beyond questioning, the underlying mechanisms responsible for the impaired immune function in the diabetic condition, poorly understood so far, are unknown to date.

As first line effector cells of the innate immune system, neutrophils are able to react in multiple ways to potential threats, namely through phagocytosis, degranulation, ROS release and formation of DNA-based extracellular traps (NETs) [5, 6]. Besides this essential defensive function of neutrophils, their role as regulatory elements in the healthy organism becomes more and more obvious [7]. Lately neutrophil granulocytes, formerly considered to depend mainly on glycolysis, were proven to adapt their metabolic pathways via transcriptional regulation to a changed environment [8]. During pathological condition of diabetes these adaptions include deficiency in ROS production, chemotaxis, adhesion and phagocytosis [8]. By which regulatory pathways these effects are transduced inside the cell is not fully understood to date [9]. However, recent studies showed that insulin is not only required for maintaining glucose homeostasis but also acts as an immunomodulatory hormone [9]. It can affect cytokine release and expression of adhesion molecules in leukocytes [9]. Whether these observations of insulin impacting the immune system may be mediated solely by an increased blood glucose level is currently under discussion [10].

Pigs are used as large animal models in a wide field of biomedical research [11]. Their close similarity to humans in terms of size, anatomy, diet and metabolism offers some significant benefits for diabetes research [11]. Developing pathologic alterations like diabetic retinopathy, vasculopathy and nephropathy, diabetes in pigs mimics the human diabetic phenotype much better than the commonly used rodent models do [11]. Genetic engineering made several transgenic breeding lines available for different approaches within the field of diabetes research [12]. The *INS*^{C94Y} transgenic pig model used in this study develops a stable diabetic phenotype within the first week of life, similar to permanent neonatal diabetes mellitus (PNDM) or mutant *INS* gene-induced diabetes of youth (MIDY) in humans [13]. Due to a point mutation within the insulin gene and consequential amino acid sequence (C—Y), the secretion of the protein by beta cells is impaired in these pigs [13]. Therefore, fasting and postprandial hyperglycemia is observed, rendering the model suitable to detect hyperglycemia-associated pathophysiologies [13].

Abnormal behavior of primary polymorphonuclear leukocytes (PMN) in diabetic settings was reported in humans and in experiments in mice [14, 15]. While studies in man can

display differences between diabetes patients depending on their state of glycemic control, early stages of diabetes are difficult to observe due to the insidious disease process. Hence, we used PMN from young *INS*^{C94Y} transgenic pigs and matched wild type controls with the aim to gain insight into changes in the neutrophil proteome that point to dysfunction occurring in the initial stage of diabetes.

MATERIAL AND METHODS

Sample preparation. PMN from heparinized venous whole blood of six 12 week old *INS*^{C94Y} transgenic (*INS*^{C94Y}) pigs and six age-matched wild type (wt) littermates were used in this study. In detail, neutrophils of four *INS*^{C94Y} and three wt animals underwent mass spectrometric analysis. Immunofluorescence staining was conducted at a later time with PMN of the other five individuals (two *INS*^{C94Y}, three wt). Relative amount of leukocyte subsets was determined via DiffQuick stained blood smears for all pigs and neutrophil percentages were comparable between both groups (*INS*^{C94Y} 30 ± 13%, wt 28 ± 8%; Supplementary Table 1). As novel findings in both murine models and humans suggest differences in the proteomic profile of circulating neutrophils driven by circadian rhythms [16, 17], the blood samples used in our experiments were all obtained at the same time of day. Collected data (mean ± SD) of glucose level (one hour post-prandial, *INS*^{C94Y} 360 ± 77 mg/dl, wt 80 ± 5 mg/dl; Supplementary Table 1) and body weight (*INS*^{C94Y} 27.5 ± 2.0 kg, wt 34.5 ± 5.7 kg; Supplementary Table 1) were in accordance with the values described by Renner et al. for this large animal model [13]. Sedimentation of erythrocytes was forced by a first 20 min centrifugation step (RT, 100 x g, brake off). PMN were then isolated from plasma by density gradient centrifugation (RT, 290 x g, 25 min, brake off) with Pancoll separating solution (PAN-Biotech, Aidenbach, Germany). Cells were then carefully washed (4°C, 400 x g, 10 min) in cold PBS and remaining erythrocytes were removed by two times 30 second sodium chloride (0.2% NaCl) lysis. Isotonicity of samples was restored through addition of equal parts of 1.6% NaCl. Cells were then washed (4°C, 400 x g, 10 min) and resuspended in PBS (pH 7.4).

Blood withdrawal was performed according to the German Animal Welfare Act with permission from the responsible authority (Government of Upper Bavaria), following the ARRIVE guidelines and Directive 2010/63/EU.

Magnetic activated cell sorting (MACS) for neutrophils. 1 x 10^7 PMN of 3 wt and 4 *INS*^{C94Y} transgenic pigs were incubated with neutrophil-specific anti-pig granulocyte antibody 6D10 (Bio-Rad AbD Serotec, Puchheim, Germany, isotype mouse IgG2a), diluted 1:50 in staining buffer (0.5% BSA + 2mM EDTA in PBS pH 7.2) for 20 min at 4°C. Cells were then washed and resuspended in 80 µl staining buffer before adding 20 µl of anti-mouse IgG2a/b MicroBeads (Miltenyi Biotec, Bergisch Gladbach, Germany). After 15 min of incubation at 4°C, cells were washed once again and resuspended in staining buffer without BSA. From now on only BSA-free buffers were used in order to avoid contamination with albumin in subsequent mass spectrometry analysis. LS columns (Miltenyi Biotec, Bergisch Gladbach, Germany) were placed in the magnetic field and rinsed with buffer solution. Cell suspension was applied followed by three washing steps to remove unlabeled cells. Then, the column was removed from the magnetic field and the positive fraction was eluted with 5 ml buffer solution. After washing twice (4°C, 300 x g, 10 min) cells were resuspended in 1 ml buffer. Successful enrichment of neutrophils was monitored by DiffQuick stained cytoslides. From each animal used in the experiment, 6 x 10^5 cells were pelleted (4°C, 2300 x g, 10 min) and stored at -20°C for filter-aided sample preparation (FASP).

Mass spectrometric analysis. Each cell pellet was directly lysed in urea buffer (8M in 0.1M Tris/HCl pH 8.5) assisted by sonication and vortexing. Samples were proteolysed with LysC and trypsin by a modified filter-aided sample preparation (FASP) as described [18]. Acidified eluted peptides were analyzed on a Q Exactive HF-X mass spectrometer (Thermo Fisher Scientific, Waltham, MA, USA) in the data-independent mode. Approximately 0.5 µg per sample spiked with one injection unit of the hyper reaction monitoring (HRM) calibration kit (Biognosys, Schlieren, Switzerland, cat. no. Ki-3003) for retention time indexing were automatically loaded to the online coupled ultra-high-performance liquid chromatography (UHPLC) system (Ultimate 3000, Thermo Fisher Scientific). A nano trap column was used (300-µm ID X 5mm, packed with Acclaim PepMap100 C18, 5 µm, 100 Å; LC Packings, Sunnyvale, CA) before separation by reversed phase chromatography (Acquity UHPLC M-Class HSS T3 Column 75 µm ID X

250 mm, 1.8 µm; Waters, Eschborn, Germany) at 40°C. Peptides were eluted from the column at 250 nL/min using increasing ACN concentration (in 0.1% formic acid) from 3% to 41% over a linear 105-min gradient. The DIA method consisted of a survey scan from 300 to 1650 mass-to-charge ratio at 120,000 resolution and an automatic gain control (AGC) target of 3e6 or 120 ms maximum injection time. Fragmentation was performed with higher energy collisional dissociation and a target value of 3e6 ions determined with predictive AGC. Precursor peptides were isolated with 37 variable windows spanning from 300 to 1650 mass-to-charge ratio at 30,000 resolution with an AGC target of 3e6 and automatic injection time. The normalized collision energy was 28, and the spectra were recorded in profile mode. The cycle times were 2.16 s and an average of seven data points for quantification per peak was reached.

For label-free quantification of DIA data, the DIA LC-MS/MS data set was analyzed by comparing the MS2 fragment spectra from the recorded windows (see above) against a spectral library collected from data-dependent acquisition data (30 raw files, derived from high pH fractionated porcine granulocytes and lymphocytes) from the same instrument. The spectral library was generated directly in Spectronaut Pulsar X (Biognosys, Schlieren, Switzerland; version 12.0.20491.17.25792) as described [19]. Spectronaut was equipped with the Ensembl Pig database (Release 75 (Sscrofa10.2), 25,859 sequences, https://www.ensembl.org) containing additional few spiked peptides (e.g., Biognosys HRM peptide sequences). The default settings for database match included: full trypsin cleavage, peptide length of between 7 and 52 amino acids and maximally two missed cleavage sites. Carbamidomethylation of cysteine was set as fixed modification and variable modifications allowed were deamidation and oxidation of methionine. All FDRs were set as 0.01 for the peptide-spectrum match (PSM), peptide and protein. To be included into the final ion library, fragment ions were required to contain a minimum of three amino acids in length, with a mass range between 300 and 1800 m/z, and a minimum relative intensity of 5%. The best 3-6 fragments per peptide were included in the library. The final spectral library generated in Spectronaut contained 4511 protein groups and 62,248 peptide precursors.

Quantification was based on cumulative MS2 area levels. Briefly, raw files were imported into Spectronaut and XIC extraction settings were set to dynamic with a correction factor

of one. Normalization was performed by default settings in Spectronaut, based on the Local Regression Normalization [20]. Automatic calibration mode was chosen with nonlinear local retention time recalibration based on the spiked HRM peptides enabled. Interference correction on MS1 and MS2 level was enabled. Peptide identification was filtered to satisfy an FDR of 1% by the mProphet approach [21]. Only proteotypic peptides were considered for protein quantification applying summed precursor quantities based on MS2 area quantity. A match between runs was enabled with the q-value percentile mode 0.3 threshold. This setting filters for peptides that fulfill the 1% FDR threshold in at least 30% of all samples.

Data availability. The mass spectrometry proteomics data have been deposited to the ProteomeXchange Consortium via the PRIDE [22] partner repository under the Project Name "The porcine granulocyte proteome: expression changes in a transgenic pig model for diabetes" with the dataset identifier PXD017274.

Data analysis. Proteins with an *INS*^{C94Y}/WT ratio of at least 2 were considered differentially abundant. Statistical analysis was performed on $\log_2$ transformed normalized abundance values using Student's *t*-test. Changes in protein abundance between conditions were considered significant at $p < 0.05$.
Heatmap was created with open source software Cluster 3.0 with the following settings: hierarchical clustering, euclidean distance for both genes and arrays, complete linkage; and was illustrated via Java TreeView (version 1.1.6r4, http://jtreeview.sourceforge.net) [23]. Volcano plot was designed with GraphPad Prism Software (version 5.04). Pathway enrichment analysis was done with open source software Reactome (Pathway Browser version 3.6, https://reactome.org) [24].

Immunofluorescence staining. 8 x 10^4 PMN of two *INS*^{C94Y} transgenic animals and three control were centrifuged (600 x g, 8 min) on microscope slides, fixed in icecold acetone and air dried or directly stored at -20°C for later analysis. After rehydration in TBS-T for 15 min, blocking was performed with 5% goat serum (in TBS-T) for 40 min. Primary antibody (polyclonal rabbit anti-human MYL9 antibody, Dianova, Hamburg

Germany) was diluted 1:100 in staining buffer (TBS-T containing 1% BSA) and incubated with cells at 4°C overnight. As specified by the manufacturer, cross reactivity of this antibody was expected and sequence homology of porcine myosin regulatory light chain 9 with human protein was checked via BLASTP (version 2.10.0+, 99.42% identities, E-value 1e-125) [25, 26]. In western blot the antibody revealed a strong signal at the level of 15 kDa and two discreet bands at 10 and 18 kDa.

Following three washing steps with staining buffer, secondary antibody (goat anti-rabbit IgG H+L Alexa568, Invitrogen, Karlsruhe, Germany; 1:500) was applied for 30 minutes. Cell nuclei were counterstained with 4′,6-diamidino-2-phenylindole (DAPI, Invitrogen, Karlsruhe, Germany; 1:1000) and slides were mounted with coverslips using mounting medium. Binding pattern of polyclonal MYL9-antibody on PMN was assessed using a Leica Dmi8 microscope with associated LAS-X-software (both Leica, Wetzlar, Germany). Grey value of 71 (wt, n=3) and 51 single cells (*INS*^{C94Y}, n=2), respectively, was determined and statistics was calculated on mean factors of intensity with GraphPad Prism Software (version 5.04) using Mann-Whitney U-test.

RESULTS

The porcine neutrophil proteome shows divergent protein abundances in *INS*^{C94Y} transgenic pigs. We identified a total of 2371 proteins in the whole sample set of primary pig neutrophils (Supplementary Table 2). Of these, 1680 were identified with at least two unique peptides. The cell fraction analyzed here consisted of 98.4 ± 1.9% neutrophils with lymphocytes being the most frequent impurity (1.2 ± 1.2%, Supplementary Fig. 1C). Quantitative comparison of the protein repertoire revealed 51 proteins with significant differences in abundance between *INS*^{C94Y} transgenic animals and control group (Table 1). Whereas 18 proteins were higher abundant in wild type, 33 showed increased abundances in diabetic pigs compared to controls. To further illustrate the quantifications, we performed hierarchical cluster analysis with the differentially abundant proteins. As visualized in Fig. 1, each individual sample clustered to its correct group (wt or *INS*^{C94Y}).

Five proteins display significantly increased abundances in neutrophils of diabetic pigs. Due to the fact that only 2-fold protein abundance differences were considered

biologically relevant, value for *INS*^{C94Y}/wt ratio cut-off was set at ≥2 for further analysis. Among the 51 differentially abundant proteins, eight passed this threshold (Fig. 2). Out of these, five candidates were identified with at least two unique peptides. At the top of this list, COP9 signalosom subunit 2 (SGN2) was 10-fold higher abundant in neutrophils of diabetic pigs, followed by myosin regulatory light chain 9 (MLC-2C, ratio 4.6) and myxovirus resistance protein 1 (ratio 3.8). The protein abundance of the open reading frame 43 on chromosome 19 (C19orf43) showed a 2.8-fold increase in *INS*^{C94Y} transgenic pigs compared to controls. Further, advillin was identified with a 2.4-fold higher abundance in neutrophil granulocytes of diabetic pigs.

Since two of these enriched proteins (myosin regulatory light chain 9 and advillin) are related to cytoskeletal dynamics and alterations of this crucial process in granulocytes are known to affect immune defense [27], we focused our further experiments on myosin regulatory light chain 9, which had the higher fold change compared to advillin.

Immunocytology highlights myosin regulatory light chain 9 abundance differences in PMN of diabetic pigs. To further characterize myosin regulatory light chain 9 in PMN of diabetic pigs, we performed immunofluorescence staining (Fig. 3). As shown by representative immunofluorescence images, myosin regulatory light chain 9 was detected in most of the mapped PMN both in wild type and diabetic pigs (Fig. 3B, D). Regarding the subcellular location, myosin regulatory light chain 9 seems to be associated to a perinuclear region to a similar extent in both groups. However, myosin regulatory light chain 9 level was increased 4-fold (**** $p < 0.0001$) in cells from *INS*^{C94Y} transgenic pigs compared to controls (Fig. 3E).

DISCUSSION

Using label-free LC-MS/MS, we obtained a proteomic data set for porcine neutrophils with an unprecedented high resolution of 2371 identified proteins. Hence our data provide a basis for further research regarding the innate immune system of pigs. Moreover, the aim of the present study was to characterize neutrophil granulocytes in *INS*^{C94Y} transgenic pigs and gain deeper insight into proteomic changes related to the early stage of diabetes mellitus. 51 of all identified proteins differed significantly in abundances between the

diabetic group and controls. Our findings match well with results from recent studies in humans on this matter, describing 30 differences in the PMN proteome from diabetic patients compared to healthy controls [15]. While 18 of our identified proteins were also among the 30 identifications from the human dataset, none of these 18 proteins reached the set ratio cut-off of 2, which we applied to satisfy stringency. This may originate from the use of different methodology: analysis of human specimen was performed with 2D-gelelectrophoresis, as opposed to our non-gel-based approach [15]. Further, the gel-based experiments of the human study were performed on a mixed population of neutrophils, eosinophils and basophils, and only included significantly altered spots in subsequent mass spectrometry analysis [15], whereas we specifically targeted neutrophils for proteome analysis in *INS*^{C94Y} transgenic pigs and controls. In order to ensure purity of neutrophils used in our experiments, we performed magnetic activated cell sorting with a porcine specific antibody which binds to an antigen exclusively expressed on neutrophil granulocytes [28]. However, the amount of this antigenic surface molecule decreases in the course of neutrophil maturation [28]. Interestingly, we could observe evidence of this process in our sorting experiment, as the positive fraction of sorted cells consisted of both immature, banded and mature, segmented neutrophils, while the flow-through contained distinctly mature neutrophils showing nuclei with more than four lobes (Supplementary Fig. 1). Therefore, our mass spectrometry data set represents the porcine proteome of 6D10-antigen positive neutrophils in the peripheral blood.

The protein with the highest statistically significant fold change in transgenic animals was subunit 2 of COP9 (SGN2, Fig. 2, Table 1). The ubiquitous, highly conserved eight-subunit protein complex COP9 signalosome (CSN) predominantly controls proteolysis via the ubiquitin-proteasome pathway by influencing the activity of cullin-RING ubiquitin ligases (CRLs) [29]. Recent findings identified SGN2 as binding partner of the cofactor IP_6, recruiting CRLs and thereby strengthening the CRL-CSN interaction [30]. CSN's contribution to regulatory processes in innate immune system is mediated by the universal transcription factor NF-κB, more precisely through the destabilization of its inhibitor IκBα [31]. Since bound IκBα masks the nuclear localization sequence of NF-κB, the complex remains in the cytosol of unstimulated cells [32]. Phosphorylation of the

inhibitor by an IκB kinase (IKK) complex triggers IκBα ubiquitination by an active CRL and subsequent degradation by 26S-proteasome [29]. Requiring NEDDylated cullin for their active form, CRLs are inhibited by deNEDDylation via CSN leading to impeded induction of NF-κB target genes [29]. Increased NF-κB activity in type 1 diabetic patients was already described in various studies and different cells [33, 34]. For instance, positive correlation of NF-κB activation with the quality of glycemic control (indicated by HbA1c) was demonstrated for peripheral blood mononuclear cells (PBMC) by Electrophoretic Mobility Shift Assay (EMSA) technique [33] and RT-PCR [35]. Although blood glucose levels of the *INS*^{C94Y} transgenic animals were elevated over a period of several weeks [13], NF-κB abundance in neutrophils of the diabetic animals was slightly lower compared to control group in our dataset (ratio 0.9, Table 1), which needs further assessment.

Besides SGN2, a second protein related to NF-κB signaling was higher abundant in *INS*^{C94Y} transgenic pigs. Gene product of C19orf43, a protein molecule first described in 2017 as interacting part of the human telomerase RNA and therefore named telomerase RNA interacting RNAse (TRIR) [36], showed 3-fold higher abundance compared to neutrophils of control group (Fig. 2, Table 1). Although little is known about its exact function, Park et al. proved that overexpression of TRIR inhibits protein phosphatase 4 (PP4) activity in numerous cell lines [37]. By dephosphorylating its target substrates, PP4 is implicated in various cellular processes, such as stem cell development, glucose metabolism, cell migration and immune response [37]. Thus, PP4 inactivates the IKK complex and subsequently acts as negative regulator for NF-κB [38]. But also the opposite effect of PP4 on NF-κB signaling was proven, suggesting a multifaceted role of this phosphatase in cellular physiology [37]. This hypothesis is supported by the observation of Zhan et al. that PP4 suppressed virus-induced type I IFN production in peritoneal macrophages [39]. In reverse, higher abundance of physiological PP4-inhibitor exoribonuclease TRIR in neutrophils of *INS*^{C94Y} transgenic pigs might be responsible for increasing IFNα levels. This cytokine recently emerged as a major trigger in the early state of type 1 diabetes generating an inflammatory milieu facilitating the diabetogenic adaptive immune response [40]. Although the diabetic condition of the studied animals was initiated by genetic engineering, our proteomic data nevertheless shows correlation to elevated IFNα, namely through identification of myxovirus resistance protein 1, a IFN-

induced dynamin-like GTPase related to the interferon stimulated genes (ISGs) [41], which was 4-fold higher abundant in *INS*^{C94Y} neutrophils compared to controls (Fig. 2, Table 1). Usually expression of ISGs increases as part of the antiviral immune defense mechanism [42, 43]. High levels of myxovirus resistance protein 1 in *INS*^{C94Y} neutrophils might therefore point to increased production and activation of type I IFNs through enhanced TLR signaling in early stage diabetes. However, its exact role in this context remains elusive and merits further investigations.

A further protein with increased abundance in *INS*^{C94Y} neutrophils, advillin (ratio 2.1, Fig. 2, Table 1), belongs to the villin/gelsolin superfamily and contributes to filopodia formation, ciliogenesis and cell motility [44]. Experimental overexpression of advillin in podocytes and gelsolin in fibroblasts increases their migration rate [45, 46], a phenomenon also described for gelsolin family-capping proteins in pancreatic cancer cells [47]. Accordingly, we would expect PMN of transgenic animals to show higher motility than cells of control pigs, which stands contradictory to the hypothesis of impaired immune cell function in diabetes mellitus, suggesting a two-faced role of the innate immune system in this disease. Resolving this contradiction requires functional testing of PMN *in vitro* by migration assays, which we aim to perform in future experiments.

In the present study, we focused on myosin regulatory light chain 9, subunit of nonmuscle myosin II (NMII), which was significantly increased in diabetic pigs compared to controls (Fig. 2, Table 1). NMII exists in almost all cell types and contributes to cell migration, adhesion, intracellular transport, organelle morphogenesis and actin cytoskeletal dynamics [48]. Phosphorylation of myosin regulatory light chain 9 by multiple kinases results in both enhanced ATPase activity of NMII and intensified association with actin filaments [49]. Higher expression of MYL9 was reported in skeletal muscle of myostatin-knockout pigs suspecting a regulative function in muscle energy metabolism [50]. The Human Proteome Atlas (https://www.proteinatlas.org/ version 19.1) cites MYL9 with higher expression in neutrophils and eosinophils compared to other blood cell types [51]. Quantitative analysis of immunostaining with MYL9 antibody on unsorted PMN (Fig. 3) correlated with the results of mass spectrometry confirming higher abundance of myosin regulatory light chain 9 in neutrophils of diabetic *INS*^{C94Y} transgenic pigs compared to wild type controls.

Higher expression of MYL9 related to diabetic condition was reported solely in gastric smooth muscle of mice and humans, where the meaning is still uncertain [52]. In the context of immune cell function, interaction of myosin regulatory light chain 9 with early activation marker CD69 promoted migration of T cells into inflamed lung tissue [53]. Thereby the authors obtained so called “MYL9 nets”, extracellular structures released by platelets during activation inside of blood vessels [53]. Former proteomic work detected myosin regulatory light chain 3, but not myosin regulatory light chain 9 in secretory vesicles of neutrophil granulocytes [54]. The significantly higher abundance of myosin regulatory light chain 9 in neutrophils of diabetic pigs is a novel and interesting finding and deserves further investigation to clarify its functional relevance in our opinion. First pathway enrichment analyses with all identified proteins, divided into two groups (enriched vs. diminished in *INS*^{C94Y}), revealed functional association of enriched *INS*^{C94Y} PMN proteins to neutrophil degranulation (Supplementary Table 3). Ten of the 51 significantly differential abundant proteins in this study were linked to this biological process (Table 1), pointing to an aberrant function of the innate immune system in the initial stage of diabetes in response to sustained hyperglycemia.

CONCLUSION

Our study provides novel information on the proteome of porcine neutrophil granulocytes in general and shows that significant changes can be detected in an initial stage of diabetes mellitus in a transgenic diabetic pig model. We gained insights into the differentiated reaction of neutrophil proteome to permanently elevated blood glucose levels. Further experiments are needed to elucidate the exact role of the different abundant candidates and especially myosin regulatory light chain 9 in the context of altered innate immune cell function in diabetes.

AUTHOR CONTRIBUTIONS

C.D. conceived and designed the experiment; M.W., C.D., B.A. and S.M.H. performed the experiments and analyzed the data; S.R. and E.W. contributed reagents, materials and analysis tools; M.W., R.D. and C.D. wrote the manuscript. All authors critically read the manuscript and approved the final version to be published.

COMPETING INTERESTS

The authors declare that they have no competing interests.

ACKNOWLEDGEMENT

The authors would like to thank Carmen Wiedemann, Bernhard Hobmaier and Isabella Giese for critical discussions and for assistance in blood sampling.

TABLES

Table 1. Proteins showing significant differences in abundance between *INS*^{C94Y} transgenic pigs and non-transgenic controls. Column 1 (protein ID) contains the accession number of the identified protein and column 2 (description) the respective protein name, both as listed in the Ensembl protein database (http://www.ensembl.org). Italicized names display proteins originally listed as uncharacterized protein in the Ensembl database output. Searching by accession number in the Universal Protein Resource database (https://www.uniprot.org) provided the description for these proteins. Column 3 (gene name) contains the name of the human orthologue gene. Column 4 (ratio) shows ratio of protein abundance in *INS*^{C94Y} transgenic pigs compared to the control group. The p-value as calculated by Student's *t*-test is shown in column 5. Column 6 (peptide counts) displays the number of unique peptides used for quantification. Highlighted proteins are assigned to the process of neutrophil degranulation by pathway enrichment analysis in the Reactome Knowledgebase (https://reactome.org).

FIGURES

Fig. 1. Hierarchical clustering of proteins with a significance level $p < 0.05$ for comparison of protein abundances between *INS*^{C94Y} transgenic pigs and non-transgenic controls. Yellow color indicates decreased and blue color increased abundance of the identified proteins labeled on the right with their human orthologue gene names. Each individual animal was assigned to its respective group by unsupervised clustering.

Fig. 2. Volcano plot of the 2371 proteins identified by differential proteome analysis. Candidates with significant ($p < 0.05$) fold change (ratio > 2) which were identified by at least two unique peptides are marked blue and labeled with their human orthologue gene name.

Fig. 3. Immunofluorescence staining of PMN for myosin regulatory light chain 9. Representative images of a control (A, B) and an *INS*^{C94Y} transgenic (C, D) pig are shown. Differential interference contrast (DIC) image of each slide is displayed on the left and the corresponding section as overlay of myosin regulatory light chain 9 (red) and nucleus (blue, counterstained with DAPI) on the right. Intracellular distribution of myosin regulatory light chain 9 was similar in both groups and restricted to a perinuclear region (enlarged section in B, D). Signal intensity of myosin regulatory light chain 9 was significantly (**** $p < 0.0001$) higher in *INS*^{C94Y} transgenic pigs compared to controls (E). Bars represent means of 71 (control) and 51 (*INS*^{C94Y}) single cell values of three (control), respectively two (*INS*^{C94Y}) individuals.

References

[1] I.D.F. I, IDF Diabetes Atlas, International Diabetes Federation (IDF), Brüssel (2019).

[2] P. Saeedi, I. Petersohn, P. Salpea, B. Malanda, S. Karuranga, N. Unwin, S. Colagiuri, L. Guariguata, A.A. Motala, K. Ogurtsova, J.E. Shaw, D. Bright, R. Williams, I.D.F.D.A. Committee, Global and regional diabetes prevalence estimates for 2019 and projections for 2030 and 2045: Results from the International Diabetes Federation Diabetes Atlas, 9(th) edition, Diabetes Res Clin Pract 157 (2019) 107843.

[3] A. Toniolo, G. Cassani, A. Puggioni, A. Rossi, A. Colombo, T. Onodera, E. Ferrannini, The diabetes pandemic and associated infections: suggestions for clinical microbiology, Rev Med Microbiol 30(1) (2019) 1-17.

[4] J. Smit, M. Sogaard, H.C. Schonheyder, H. Nielsen, T. Froslev, R.W. Thomsen, Diabetes and risk of community-acquired Staphylococcus aureus bacteremia: a population-based case-control study, European journal of endocrinology 174(5) (2016) 631-9.

[5] M. van der Linden, L. Meyaard, Fine-tuning neutrophil activation: Strategies and consequences, Immunol Lett 178 (2016) 3-9.

[6] N. de Buhr, M.C. Bonilla, M. Jimenez-Soto, M. von Kockritz-Blickwede, G. Dolz, Extracellular Trap Formation in Response to Trypanosoma cruzi Infection in Granulocytes Isolated From Dogs and Common Opossums, Natural Reservoir Hosts, Front Microbiol 9 (2018) 966.

[7] M. Casanova-Acebes, J.A. Nicolás-Ávila, J.L. Li, S. García-Silva, A. Balachander, A. Rubio-Ponce, L.A. Weiss, J.M. Adrover, K. Burrows, N. A-González, I. Ballesteros, S. Devi, J.A. Quintana, G. Crainiciuc, M. Leiva, M. Guzzer, C. Weber, T. Nagasawa, O. Soehnlein, M. Merad, A. Mortha, L.G. Ng, H. Peinado, A. Hidalgo, Neutrophils instruct homeostatic and pathological states in naive tissues, The Journal of experimental medicine 215(11) (2018) 2778-2795.

[8] S. Kumar, M. Dikshit, Metabolic Insight of Neutrophils in Health and Disease, Frontiers in immunology 10 (2019) 2099-2099.

[9] G. van Niekerk, C. Christowitz, D. Conradie, A.M. Engelbrecht, Insulin as an immunomodulatory hormone, Cytokine Growth Factor Rev (2019).

[10] G. van Niekerk, T. Davis, H.G. Patterton, A.M. Engelbrecht, How Does Inflammation-Induced Hyperglycemia Cause Mitochondrial Dysfunction in Immune Cells?, Bioessays 41(5) (2019) e1800260.

[11] S. Renner, B. Dobenecker, A. Blutke, S. Zols, R. Wanke, M. Ritzmann, E. Wolf, Comparative aspects of rodent and nonrodent animal models for mechanistic and translational diabetes research, Theriogenology 86(1) (2016) 406-21.

[12] S. Renner, A. Blutke, S. Clauss, C.A. Deeg, E. Kemter, D. Merkus, R. Wanke, E. Wolf, Porcine models for studying complications and organ crosstalk in diabetes mellitus, Cell and Tissue Research (2020).

[13] S. Renner, C. Braun-Reichhart, A. Blutke, N. Herbach, D. Emrich, E. Streckel, A. Wunsch, B. Kessler, M. Kurome, A. Bahr, N. Klymiuk, S. Krebs, O. Puk, H. Nagashima, J. Graw, H. Blum, R. Wanke, E. Wolf, Permanent neonatal diabetes in INS(C94Y) transgenic pigs, Diabetes 62(5) (2013) 1505-11.

[14] S.L. Wong, M. Demers, K. Martinod, M. Gallant, Y. Wang, A.B. Goldfine, C.R. Kahn, D.D. Wagner, Diabetes primes neutrophils to undergo NETosis, which impairs wound healing, Nat Med 21(7) (2015) 815-9.

[15] J. Soongsathitanon, W. Umsa-Ard, V. Thongboonkerd, Proteomic analysis of peripheral blood polymorphonuclear cells (PBMCs) reveals alteration of neutrophil extracellular trap (NET) components in uncontrolled diabetes, Molecular and Cellular Biochemistry 461(1) (2019) 1-14.

[16] J.M. Adrover, A. Aroca-Crevillen, G. Crainiciuc, F. Ostos, Y. Rojas-Vega, A. Rubio-Ponce, C. Cilloniz, E. Bonzon-Kulichenko, E. Calvo, D. Rico, M.A. Moro, C. Weber, I. Lizasoain, A. Torres, J. Ruiz-Cabello, J. Vazquez, A. Hidalgo, Programmed 'disarming' of the neutrophil proteome reduces the magnitude of inflammation, Nat Immunol 21(2) (2020) 135-144.

[17] J.M. Adrover, C. del Fresno, G. Crainiciuc, M.I. Cuartero, M. Casanova-Acebes, L.A. Weiss, H. Huerga-Encabo, C. Silvestre-Roig, J. Rossaint, I. Cossío, A.V. Lechuga-Vieco, J. García-Prieto, M. Gómez-Parrizas, J.A. Quintana, I. Ballesteros, S. Martin-Salamanca, A. Aroca-

Crevillen, S.Z. Chong, M. Evrard, K. Balabanian, J. López, K. Bidzhekov, F. Bachelerie, F. Abad-Santos, C. Muñoz-Calleja, A. Zarbock, O. Soehnlein, C. Weber, L.G. Ng, C. Lopez-Rodriguez, D. Sancho, M.A. Moro, B. Ibáñez, A. Hidalgo, A Neutrophil Timer Coordinates Immune Defense and Vascular Protection, Immunity 50(2) (2019) 390-402.e10.

[18] A. Grosche, A. Hauser, M.F. Lepper, R. Mayo, C. von Toerne, J. Merl-Pham, S.M. Hauck, The Proteome of Native Adult Muller Glial Cells From Murine Retina, Mol Cell Proteomics 15(2) (2016) 462-80.

[19] J. Singh, E. Kaade, J. Muntel, R. Bruderer, L. Reiter, M. Thiel, D. Winter, Systematic Comparison of Strategies for the Enrichment of Lysosomes by Data Independent Acquisition, J Proteome Res 19(1) (2020) 371-381.

[20] S.J. Callister, R.C. Barry, J.N. Adkins, E.T. Johnson, W.J. Qian, B.J. Webb-Robertson, R.D. Smith, M.S. Lipton, Normalization approaches for removing systematic biases associated with mass spectrometry and label-free proteomics, J Proteome Res 5(2) (2006) 277-86.

[21] L. Reiter, O. Rinner, P. Picotti, R. Hüttenhain, M. Beck, M.Y. Brusniak, M.O. Hengartner, R. Aebersold, mProphet: automated data processing and statistical validation for large-scale SRM experiments, Nat Methods 8(5) (2011) 430-5.

[22] Y. Perez-Riverol, A. Csordas, J. Bai, M. Bernal-Llinares, S. Hewapathirana, D.J. Kundu, A. Inuganti, J. Griss, G. Mayer, M. Eisenacher, E. Perez, J. Uszkoreit, J. Pfeuffer, T. Sachsenberg, S. Yilmaz, S. Tiwary, J. Cox, E. Audain, M. Walzer, A.F. Jarnuczak, T. Ternent, A. Brazma, J.A. Vizcaino, The PRIDE database and related tools and resources in 2019: improving support for quantification data, Nucleic Acids Res 47(D1) (2019) D442-D450.

[23] M.J. de Hoon, S. Imoto, J. Nolan, S. Miyano, Open source clustering software, Bioinformatics 20(9) (2004) 1453-4.

[24] A. Fabregat, K. Sidiropoulos, G. Viteri, O. Forner, P. Marin-Garcia, V. Arnau, P. D'Eustachio, L. Stein, H. Hermjakob, Reactome pathway analysis: a high-performance in-memory approach, BMC Bioinformatics 18(1) (2017) 142.

[25] S.F. Altschul, T.L. Madden, A.A. Schaffer, J. Zhang, Z. Zhang, W. Miller, D.J. Lipman, Gapped BLAST and PSI-BLAST: a new generation of protein database search programs, Nucleic Acids Res 25(17) (1997) 3389-402.

[26] S.F. Altschul, J.C. Wootton, E.M. Gertz, R. Agarwala, A. Morgulis, A.A. Schaffer, Y.K. Yu, Protein database searches using compositionally adjusted substitution matrices, The FEBS journal 272(20) (2005) 5101-9.

[27] S.S. Parikh, S.A. Litherland, M.J. Clare-Salzler, W. Li, P.A. Gulig, F.S. Southwick, CapG(-/-) mice have specific host defense defects that render them more susceptible than CapG(+/+) mice to Listeria monocytogenes infection but not to Salmonella enterica serovar Typhimurium infection, Infect Immun 71(11) (2003) 6582-6590.

[28] C. Perez, C. Revilla, B. Alvarez, S. Chamorro, C. Correa, N. Domenech, F. Alonso, A. Ezquerra, J. Dominguez, Phenotypic and functional characterization of porcine granulocyte developmental stages using two new markers, Dev Comp Immunol 31(3) (2007) 296-306.

[29] G.A. Cope, R.J. Deshaies, COP9 signalosome: a multifunctional regulator of SCF and other cullin-based ubiquitin ligases, Cell 114(6) (2003) 663-71.

[30] H. Lin, X. Zhang, L. Liu, Q. Fu, C. Zang, Y. Ding, Y. Su, Z. Xu, S. He, X. Yang, X. Wei, H. Mao, Y. Cui, Y. Wei, C. Zhou, L. Du, N. Huang, N. Zheng, T. Wang, F. Rao, Basis for metabolite-dependent Cullin-RING ligase deneddylation by the COP9 signalosome, Proc Natl Acad Sci U S A 117(8) (2020) 4117-4124.

[31] K. Schweitzer, M. Naumann, Control of NF-kappaB activation by the COP9 signalosome, Biochem Soc Trans 38(Pt 1) (2010) 156-61.

[32] T.T. Huang, N. Kudo, M. Yoshida, S. Miyamoto, A nuclear export signal in the N-terminal regulatory domain of IkappaBalpha controls cytoplasmic localization of inactive NF-kappaB/IkappaBalpha complexes, Proc Natl Acad Sci U S A 97(3) (2000) 1014-9.

[33] M.A. Hofmann, S. Schiekofer, B. Isermann, M. Kanitz, M. Henkels, M. Joswig, A. Treusch, M. Morcos, T. Weiss, V. Borcea, A.K. Abdel Khalek, J. Amiral, H. Tritschler, E. Ritz, P. Wahl, R. Ziegler, A. Bierhaus, P.P. Nawroth, Peripheral blood monocytic cells isolated from patients with diabetic nephropathy show increased activation of the oxidative-stress sensitive transcription factor NF-kappaB, Diabetologia 42(2) (1999) 222-32.

[34] J. Trinanes, E. Salido, J. Fernandez, M. Rufino, J.M. Gonzalez-Posada, A. Torres, D. Hernandez, Type 1 diabetes increases the expression of proinflammatory cytokines and adhesion molecules in the artery wall of candidate patients for kidney transplantation, Diabetes Care 35(2) (2012) 427-33.

[35] A. Bierhaus, S. Schiekofer, M. Schwaninger, M. Andrassy, P.M. Humpert, J. Chen, M. Hong, T. Luther, T. Henle, I. Kloting, M. Morcos, M. Hofmann, H. Tritschler, B. Weigle, M. Kasper, M. Smith, G. Perry, A.M. Schmidt, D.M. Stern, H.U. Haring, E. Schleicher, P.P. Nawroth, Diabetes-associated sustained activation of the transcription factor nuclear factor-kappaB, Diabetes 50(12) (2001) 2792-808.

[36] J. Xie, Z. Chen, X. Zhang, H. Chen, W. Guan, Identification of an RNase that preferentially cleaves A/G nucleotides, Sci Rep 7 (2017) 45207.

[37] J. Park, J. Lee, D.H. Lee, Identification of Protein Phosphatase 4 Inhibitory Protein That Plays an Indispensable Role in DNA Damage Response, Mol Cells 42(7) (2019) 546-556.

[38] M. Brechmann, T. Mock, D. Nickles, M. Kiessling, N. Weit, R. Breuer, W. Muller, G. Wabnitz, F. Frey, J.P. Nicolay, N. Booken, Y. Samstag, C.D. Klemke, M. Herling, M. Boutros, P.H. Krammer, R. Arnold, A PP4 holoenzyme balances physiological and oncogenic nuclear factor-kappa B signaling in T lymphocytes, Immunity 37(4) (2012) 697-708.

[39] Z. Zhan, H. Cao, X. Xie, L. Yang, P. Zhang, Y. Chen, H. Fan, Z. Liu, X. Liu, Phosphatase PP4 Negatively Regulates Type I IFN Production and Antiviral Innate Immunity by Dephosphorylating and Deactivating TBK1, J Immunol 195(8) (2015) 3849-57.

[40] A. Lombardi, E. Tsomos, S.S. Hammerstad, Y. Tomer, Interferon alpha: The key trigger of type 1 diabetes, J Autoimmun 94 (2018) 7-15.

[41] G.R. Stark, I.M. Kerr, B.R. Williams, R.H. Silverman, R.D. Schreiber, How cells respond to interferons, Annu Rev Biochem 67 (1998) 227-64.

[42] H.K. Chung, J.H. Lee, S.H. Kim, C. Chae, Expression of interferon-alpha and Mx1 protein in pigs acutely infected with porcine reproductive and respiratory syndrome virus (PRRSV), J Comp Pathol 130(4) (2004) 299-305.

[43] O. Haller, P. Staeheli, M. Schwemmle, G. Kochs, Mx GTPases: dynamin-like antiviral machines of innate immunity, Trends Microbiol 23(3) (2015) 154-63.

[44] P. Silacci, L. Mazzoni, C. Gauci, N. Stergiopulos, H.L. Yin, D. Hayoz, Gelsolin superfamily proteins: key regulators of cellular functions, Cell Mol Life Sci 61(19-20) (2004) 2614-23.

[45] J. Rao, S. Ashraf, W. Tan, A.T. van der Ven, H.Y. Gee, D.A. Braun, K. Feher, S.P. George, A. Esmaeilniakooshkghazi, W.I. Choi, T. Jobst-Schwan, R. Schneider, J.M. Schmidt, E. Widmeier, J.K. Warejko, T. Hermle, D. Schapiro, S. Lovric, S. Shril, A. Daga, A. Nayir, M. Shenoy, Y. Tse, M. Bald, U. Helmchen, S. Mir, A. Berdeli, J.A. Kari, S. El Desoky, N.A.

Soliman, A. Bagga, S. Mane, M.A. Jairajpuri, R.P. Lifton, S. Khurana, J.C. Martins, F. Hildebrandt, Advillin acts upstream of phospholipase C 1 in steroid-resistant nephrotic syndrome, J Clin Invest 127(12) (2017) 4257-4269.

[46] C.C. Cunningham, T.P. Stossel, D.J. Kwiatkowski, Enhanced motility in NIH 3T3 fibroblasts that overexpress gelsolin, Science 251(4998) (1991) 1233-6.

[47] C.C. Thompson, F.J. Ashcroft, S. Patel, G. Saraga, D. Vimalachandran, W. Prime, F. Campbell, A. Dodson, R.E. Jenkins, N.R. Lemoine, T. Crnogorac-Jurcevic, H.L. Yin, E. Costello, Pancreatic cancer cells overexpress gelsolin family-capping proteins, which contribute to their cell motility, Gut 56(1) (2007) 95-106.

[48] M. Vicente-Manzanares, X. Ma, R.S. Adelstein, A.R. Horwitz, Non-muscle myosin II takes centre stage in cell adhesion and migration, Nature reviews. Molecular cell biology 10(11) (2009) 778-90.

[49] R.S. Adelstein, M. Anne Conti, Phosphorylation of platelet myosin increases actin-activated myosin ATPase activity, Nature 256(5518) (1975) 597-598.

[50] X. Li, S. Xie, L. Qian, C. Cai, H. Bi, W. Cui, Identification of genes related to skeletal muscle growth and development by integrated analysis of transcriptome and proteome in myostatin-edited Meishan pigs, Journal of Proteomics 213 (2020) 103628.

[51] P.J. Thul, L. Akesson, M. Wiking, D. Mahdessian, A. Geladaki, H. Ait Blal, T. Alm, A. Asplund, L. Bjork, L.M. Breckels, A. Backstrom, F. Danielsson, L. Fagerberg, J. Fall, L. Gatto, C. Gnann, S. Hober, M. Hjelmare, F. Johansson, S. Lee, C. Lindskog, J. Mulder, C.M. Mulvey, P. Nilsson, P. Oksvold, J. Rockberg, R. Schutten, J.M. Schwenk, A. Sivertsson, E. Sjostedt, M. Skogs, C. Stadler, D.P. Sullivan, H. Tegel, C. Winsnes, C. Zhang, M. Zwahlen, A. Mardinoglu,

F. Ponten, K. von Feilitzen, K.S. Lilley, M. Uhlen, E. Lundberg, A subcellular map of the human proteome, Science 356(6340) (2017).

[52] W. Li, K.C. Sasse, Y. Bayguinov, S.M. Ward, B.A. Perrino, Contractile Protein Expression and Phosphorylation and Contractility of Gastric Smooth Muscles from Obese Patients and Patients with Obesity and Diabetes, J Diabetes Res 2018 (2018) 8743874-8743874.

[53] M.Y. Kimura, K. Hayashizaki, K. Tokoyoda, S. Takamura, S. Motohashi, T. Nakayama, Crucial role for CD69 in allergic inflammatory responses: CD69-Myl9 system in the pathogenesis of airway inflammation, Immunological Reviews 278(1) (2017) 87-100.

[54] S. Rørvig, O. Østergaard, N.H.H. Heegaard, N. Borregaard, Proteome profiling of human neutrophil granule subsets, secretory vesicles, and cell membrane: correlation with transcriptome profiling of neutrophil precursors, Journal of Leukocyte Biology 94(4) (2013) 711-721.

Fig. 1. Hierarchical clustering of proteins with significance level $p < 0.05$ for comparison of protein abundances between *INS*^{C94Y} transgenic pigs and non-transgenic controls. Yellow color indicates decreased and blue color increased abundance of the identified proteins labeled on the right with their human orthologue gene names. Each individual animal was assigned to its respective group by unsupervised clustering.

Fig. 2. Volcano plot of the 2371 proteins identified by differential proteome analysis. Candidates with significant ($p < 0.05$) fold change (ratio > 2) which were identified by at least two unique peptides are marked blue and labeled with their human orthologue gene name.

Fig. 3. Immunofluorescence staining of PMN for myosin regulatory light chain 9. Representative images of a control (A, B) and an *INS*^{C94Y} transgenic (C, D) pig are shown.

Differential interference contrast (DIC) image of each slide is displayed on the left and the corresponding section as overlay of myosin regulatory light chain 9 (red) and nucleus (blue, counterstained with DAPI) on the right. Intracellular distribution of myosin regulatory light chain 9 was similar in both groups and restricted to a perinuclear region (enlarged section in B, D). Signal intensity of myosin regulatory light chain 9 was significantly (**** $p < 0.0001$) higher in *INS*^{C94Y} transgenic pigs compared to controls (E). Bars represent means of 71 (control) and 51 (*INS*^{C94Y}) single cell values of three (control), respectively two (*INS*^{C94Y}) individuals.

Credit Author Statement

Cornelia A. Deeg conceived and designed the experiments, and supervised the project; **Maria Weigand, Cornelia A. Deeg, Barbara Ariann and Stefanie M. Hauck** performed the experiments and analyzed the data; **Simone Renner and Eckhard Wolf** contributed reagents, materials and analysis tools; **Maria Weigand, Roxane L. Degroote and Cornelia A. Deeg** wrote the manuscript. All authors critically read the manuscript and approved the final version to be published.

SIGNIFICANCE

Our studies provide novel basic information about the neutrophil proteome of pigs and contribute to a better understanding of molecular mechanisms involved in altered immune cell function in an early stage diabetes. We demonstrate proteins that are dysregulated in neutrophils from a transgenic diabetic pig model and have not been described in this context so far. The data presented here are highly relevant for veterinary medicine and have translational quality for diabetes in humans.

TABLES

Protein ID	Description	Gene name
ENSSSCP00000005012	COP9 signalosome subunit 2	COPS2
ENSSSCP00000026757	Sus scrofa myosin, light chain 9, regulatory	MYL9
ENSSSCP00000012965	Eukaryotic translation initiation factor 2 subunit 3	EIF2S3
ENSSSCP00000029166	Sus scrofa myxovirus (influenza virus) resistance 1, interferon-inducible protein p78 (mouse)	MX1
ENSSSCP00000008078	tweety family member 3	TTYH3
ENSSSCP00000014597	chromosome 19 open reading frame 43	C19orf43
ENSSSCP00000023779	advillin	AVIL
ENSSSCP00000024948	enoyl-CoA delta isomerase 1	ECI1
ENSSSCP00000014442	translocase of inner mitochondrial membrane 44 homolog (yeast)	TIMM44
ENSSSCP00000006805	SLAM family member 6	SLAMF6
ENSSSCP00000014722	Sus scrofa tropomyosin 4	TPM4
ENSSSCP00000022159	glyoxalase I	GLO1
ENSSSCP00000000040	cytochrome b5 reductase 3	CYB5R3
ENSSSCP00000009601	Sus scrofa fibrinogen beta chain	FGB
ENSSSCP00000012625	leucine-rich repeats and calponin homology (CH) domain containing 3	LRCH3
ENSSSCP00000014764	microtubule-associated protein 1S	MAP1S
ENSSSCP00000025078	*Sec1 family domain containing 2*	SCFD2
ENSSSCP00000002105	hexosaminidase A (alpha polypeptide)	HEXA
ENSSSCP00000025669	guanosine monophosphate reductase 2	GMPR2
ENSSSCP00000011592	adenylosuccinate synthetase isozyme 2	ADSS
ENSSSCP00000012502	structural maintenance of chromosomes 4	SMC4
ENSSSCP00000016213	retinoblastoma binding protein 5	RBBP5
ENSSSCP00000015747	RAB6C, member RAS oncogene family	RAB6C
ENSSSCP00000016804	*UDP-glucose glycoprotein glucosyltransferase 1*	UGGT1
ENSSSCP00000023332	down regulator of transcription 1, TBP-binding (negative cofactor 2)	DR1
ENSSSCP00000002190	proteasome activator complex subunit 2	PSME2
ENSSSCP00000002115	*Protein transport protein SEC23*	SEC23A
ENSSSCP00000024847	Sus scrofa lactate dehydrogenase B	LDHB
ENSSSCP00000014598	arsA arsenite transporter, ATP-binding, homolog 1 (bacterial)	ASNA1
ENSSSCP00000000520	cleavage and polyadenylation specificity factor subunit 6	CPSF6
ENSSSCP00000009333	DEAH (Asp-Glu-Ala-His) box helicase 15	DHX15
ENSSSCP00000003435	aldehyde dehydrogenase 16 family, member A1	ALDH16A1
ENSSSCP00000003404	Uncharacterized protein	BAX
ENSSSCP00000019539	Uncharacterized protein	GBE1
ENSSSCP00000013872	Sus scrofa OTU domain, ubiquitin aldehyde binding 1	OTUB1
ENSSSCP00000023695	*ATP-dependent RNA helicase A*	DHX9
ENSSSCP00000030177	Sus scrofa nuclear factor of kappa light polypeptide gene enhancer in B-cells 1	NFKB1
ENSSSCP00000011895	Uncharacterized protein	MCTS1
ENSSSCP00000007947	CSE1 chromosome segregation 1-like (yeast)	CSE1L

ENSSSCP00000008878	N-acetylglucosamine kinase	NAGK
ENSSSCP00000005510	phospholipase A2-activating protein	PLAA
ENSSSCP00000021608	Uncharacterized protein	UBR4
ENSSSCP00000002642	SMEK homolog 1, suppressor of mek1 (Dictyostelium)	PPP4R3A
ENSSSCP00000025778	Uncharacterized protein	MYO18A
ENSSSCP00000014753	*Myosin IXB*	MYO9B
ENSSSCP00000026257	major vault protein	MVP
ENSSSCP00000000801	WNK lysine deficient protein kinase 1	WNK1
ENSSSCP00000002862	*Pribosyltran domain-containing protein*	APRT
ENSSSCP00000006940	Sus scrofa farnesyl diphosphate synthase	FDPS
ENSSSCP00000026644	Uncharacterized protein	VPS13C
ENSSSCP00000011119	cleavage stimulation factor, 3' pre-RNA, subunit 2, 64kDa, tau variant	CSTF2T

Tab. 1. Proteins showing significant differences in abundance between *INS*^{C94Y} transgenic pigs and non-transgenic controls. Column 1 (protein ID) contains the accession number of the identified protein and column 2 (description) the respective protein name, both as listed in the Ensembl protein database (http://www.ensembl.org). Italicized names display proteins originally listed as uncharacterized protein in the Ensembl database output. Searching by accession number in the Universal Protein Resource database (https://www.uniprot.org) provided the description for these proteins. Column 3 (gene name) contains the name of the human orthologue gene. Column 4 (ratio) shows ratio of protein abundance in *INS*^{C94Y} transgenic pigs compared to the control group. The p-value as calculated by Student's *t*-test is shown in column 5. Column 6 (peptide counts) displays the number of unique peptides used for quantification. Highlighted proteins are assigned to the process of neutrophil degranulation by pathway enrichment analysis in the Reactome Knowledgebase (https://reactome.org).

HIGHLIGHTS

- Diabetic *INS*^{C94Y} pig neutrophils show changed proteome compared to wild type
- Higher abundant neutrophil proteins in diabetes associate to cytoskeletal dynamics
- Myosin regulatory light chain 9 abundance is 5-fold higher in *INS*^{C94Y} neutrophils
- Altered motility of neutrophils might affect sufficient immune response in diabetes